Chapter 16
Time-Reversed Vibration-Induced Particle Motion on an Elastic Plate

Abigail Smith, Sanchita Das, Samikhshak Gupta, and Vijaya V. N. Sriram Malladi

Abstract This study investigates the use of time-reversed vibration profiles to observe the motion of flat-surface beads on a two-dimensional elastic plate. Building on earlier demonstrations of object manipulation with time-reversal focusing, the present work examines how controlled flexural waveforms influence particle trajectories and displacement. An experimental setup with four modal shakers and a laser vibrometer is used to synthesize waveforms from measured impulse responses excited by chirp signals. By varying parameters such as frequency bandwidth, clipping threshold, excitation amplitude, particle position, and distance from the excitation source, energy is focused at prescribed locations on the plate. Particle motion is recorded with an overhead camera and analyzed to characterize displacement patterns and trajectory repeatability. Preliminary trials provide new insight into the feasibility of using tuned time-reversal profiles to study particle dynamics, advancing the foundation for vibration-based approaches to particle manipulation.

Keywords Time reversal · Vibration profile · Particle manipulation · Impulse response function · Flexural waveform

Introduction

The concept of reversing time has long fascinated scientists. In signal processing, time reversal (TR) has been studied since the 1960s [1], originally applied to underwater acoustic communication between submarines. TR enables wave fields to be refocused at a location distinct from their original source, allowing waves emitted from different source locations to amplify the response at a designated focal point. Initially termed *matched signal processing* [1], the concept was later popularized as *time-reversed acoustics* (or simply time reversal) in the 1990s by Fink and colleagues [2, 3]. Since then, its applications have expanded to medicine (e.g., lithotripsy for kidney stone treatment [4], transskull therapy [5]), hydrodynamics [6], nondestructive testing [7], and fundamental physics experiments [8]. In elastic media, TR has been used for structural health monitoring [7, 9], pipe communication [10], and seismic event localization [11]. A comprehensive overview is given in [12].

More recent demonstrations have popularized TR in laboratory environments. In 2017, BYU Acoustics visually illustrated TR focusing in a thin plate [13], followed by playful demonstrations using LEGO minifigures [14]. These studies showed the forward step—where an impulse is emitted from a source and recorded at a receiver—and the backward step, in which the recorded response is reversed in time and re-emitted to retrace the original path. This process results in the original source receiving a signal closely resembling the initial impulse. Extending this approach, multiple sources were employed with a single focal receiver: sequential emissions were recorded, time-reversed, and rebroadcast simultaneously. Constructive interference at the focal location produced a strong amplified response, validated in practical demonstrations such as knocking over small objects via localized TR focusing.

While TR in acoustics and elastic media has been widely studied, its application to *particle motion* remains limited. Early work in geophysics proposed TR imaging to investigate particle chaos and its suppression through wave propagation [15]. More recently, Anderson's group demonstrated elastic wave visualization using salt grains on a plate, showing that TR focusing could be achieved at pre-selected focal points. Building on this foundation, the present study investigates particle motion on an elastic plate to characterize the amplitude and effective radius of TR focusing. Elastic waves are introduced by

Abigail Smith · Sanchita Das · Samikhshak Gupta · Vijaya V. N. Sriram Malladi
Vibrations, Intelligent Testing, & Active Learning of Structures (ViTALS) Group, Department of Mechanical and Aerospace Engineering, Michigan Technological University, Houghton, MI 49931
e-mail: abrsmith@mtu.edu; sdas14@mtu.edu; sgupta14@mtu.edu; smalladi@mtu.edu

© The Author(s), under exclusive license to River Publishers 2026

Kristin B. Zimmerman, PhD (eds.), *Topics in Modal Analysis & Parameter Identification in Structural Dynamics, 2026, Vol. 8*, Conference Proceedings of the Society for Experimental Mechanics Series, https://doi.org/10.13052/rp-9788743814191

four modal shakers at the plate corners, and small beads placed on the plate surface serve as tracers of particle motion. The aim is to observe how TR focusing influences bead displacement and to determine the spatial extent of the focal region.

To this end, we developed an experimental setup that began with qualitative visualization (a splash of water), followed by a single bead, and later extended to grid-like arrangements of multiple beads. Initial results demonstrate the successful application of TR focusing for multi-particle motion. A more detailed analysis of individual particle trajectories and parameter effects is reserved for future work.

Overview of Time-reversal

Let $s(t)$ denote the source signal, $h(t)$ the impulse response of the medium between a source and a receiver, and $r(t)$ the received signal. Using Fourier transforms (denoted by capital letters), we write $X(\omega) = \mathbb{F}\{x(t)\}$. These derivations are followed from a book chapter called *Time Reversal Techniques* by Anderson *et al.* [16].

Forward step: The received signal is the convolution of the source with the medium response,

$$r(t) = (h * s)(t) = \int_{-\infty}^{\infty} h(\tau)\, s(t-\tau)\, d\tau, \tag{1}$$

which in the frequency domain becomes

$$R(\omega) = H(\omega)\, S(\omega). \tag{2}$$

Time reversal: The time-reversed signal is

$$y(t) = r_{\mathrm{TR}}(t) = r(-t), \tag{3}$$

which in the frequency domain corresponds to

$$Y(\omega) = R(-\omega), \quad \text{and if } r(t) \in \mathbb{R}, \quad Y(\omega) = R^*(\omega). \tag{4}$$

Backward step: Re-emitting $y(t)$ from the original source location forces multipath components to arrive in phase at the receiver (the focal point). The focal waveform is proportional to the autocorrelation of the impulse response:

$$p_{\mathrm{focus}}(t) \;\propto\; (h * h^-)(t) = \int_{-\infty}^{\infty} h(\tau)\, h(\tau - t)\, d\tau, \quad h^-(t) \equiv h(-t), \tag{5}$$

which has a sharp peak at $t = 0$. In the frequency domain,

$$P_{\mathrm{focus}}(\omega) \;\propto\; H(\omega)\, H^*(\omega) = |H(\omega)|^2. \tag{6}$$

These relations assume that the medium is linear, reciprocal, and time-invariant, with sufficient bandwidth and signal-to-noise ratio, and negligible change between forward and backward steps.

Finally, for discrete signals, if $r[n]$ has length N, then the time-reversed sequence is $r_{\mathrm{TR}}[n] = r[N-1-n]$, and for real-valued $r[n]$, the frequency-domain representation satisfies $R_{\mathrm{TR}}[k] = R^*[k]$.

Overview of Experimental Setup

The elastic medium employed in this study is a flexible aluminum plate with dimensions $9.5 \times 9.5 \times 0.06$ in^3, as shown in fig. 1a. The plate is supported at its four corners by nylon stingers that are coupled to modal shakers. Each shaker is mounted in a 3D-printed stand with bolt holes, allowing secure attachment to the test table or other fixtures. The entire assembly is stabilized by a rectangular frame constructed from 80/20 aluminum beams, which provides both portability and adjustable shaker placement. This mechanical configuration ensures that the excitation is applied in a repeatable and controlled manner.

The excitation signal is supplied by Douk Audio Nobsound power amplifiers, which are connected through custom-modified audio jacks to the data acquisition (DAQ) system. The output signals are delivered to the shakers and simultaneously looped back into the DAQ, which allows us to monitor the input and verify that any observed disturbances arise from the mechanical system rather than electrical interference. To further validate the input, PCB force sensors are positioned between the stingers and the plate, enabling direct measurement of the transmitted force. These measurements help us track the excitation as it passes through the system and isolate potential sources of noise.

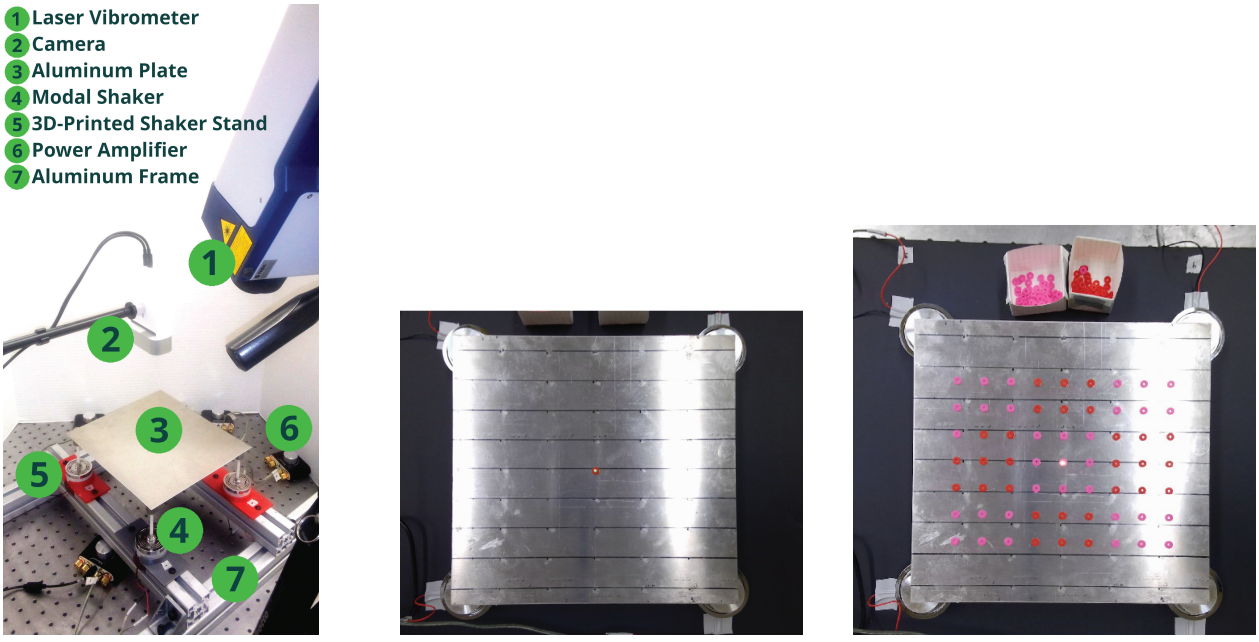

(a) (b) (c)

Fig. 1 Photographs of the experimental setup: (a) labeled view of components, (b) single particle, (c) grid-like layout of multiple particles

We record the vibrations of the plate using a Polytec MLV-100 laser vibrometer mounted on a tripod and directed toward predefined measurement points. The vibrometer output is processed by a Polytec OFV-5000 controller, which provides a velocity signal to the DAQ. To complement these measurements, we also monitor particle motion on the plate surface using a Microsoft Azure Kinect camera suspended overhead. The Kinect is connected to the control computer via USB and provides both images and videos of particle trajectories, giving us a visual record to correlate with vibrometer data.

The baseline testing procedure follows the two-step TR framework described in eqs. (1), (3) and (5). In the forward step, we generate a chirp signal in MATLAB and deliver it sequentially to the shakers while recording the response at the desired focal location using the vibrometer. This measurement provides the effective impulse response of the system, $h(t)$, convolved with the source signal. The recorded response is then processed: it is transformed into the frequency domain, windowed to reduce noise, and then time-reversed by spectral conjugation as expressed in eq. (4). In the backward step, the time-reversed signals are simultaneously re-emitted from all shakers. By reciprocity, the multipath components of the wave field retrace their original trajectories and arrive in phase at the focal point. The reconstructed waveform is therefore proportional to the autocorrelation of the impulse response, $(h * h^{-})(t)$, as in eq. (5), which produces a sharp focus in both time and space at the chosen measurement location. This two-step process provides a controlled basis for TR focusing on the plate.

With this baseline established, we extend the setup to investigate particle motion under TR focusing. The particles used are small, flat, disk-shaped rubber beads. For single particle motion (SPM), the setup requires only minor modification: as shown in fig. 1b, a single bead is placed at the focal point between the forward and backward steps. We then activate the backward step and observe the resulting displacement of the particle. For multiple particle motion (MPM), we place a total of 63 beads in a 7×9 grid layout using a plexiglass spacer to ensure precise and repeatable placement (fig. 1c). To improve clarity during analysis, beads in different regions are assigned contrasting colors.

Results and Discussion

Particle motion was further explored in a set of two trials, which were performed using the same parameters to test repeatability of the process. Each trial repeated the backward step of the TR focusing process multiple times without resetting the beads to their initial positions. This procedure was performed ten times in sequence for each trial, with the final bead positions captured after each iteration using the Microsoft Azure Kinect camera. The recorded images were processed through a

systematic pipeline: blob analysis was first applied to identify bead positions, an HSV color-thresholding method was used to create binary masks, and the Hungarian algorithm was employed to assign unique IDs and track each of the 63 beads across frames. For clarity, each processed image is referred to as a *frame*, with the initial configuration being Frame 1. Including the ten repeated backward steps, the dataset comprised 11 frames. Representative examples—Frames 1, 3, 5, 7, 9, and 11—from Trial 1 are shown in fig. 2.

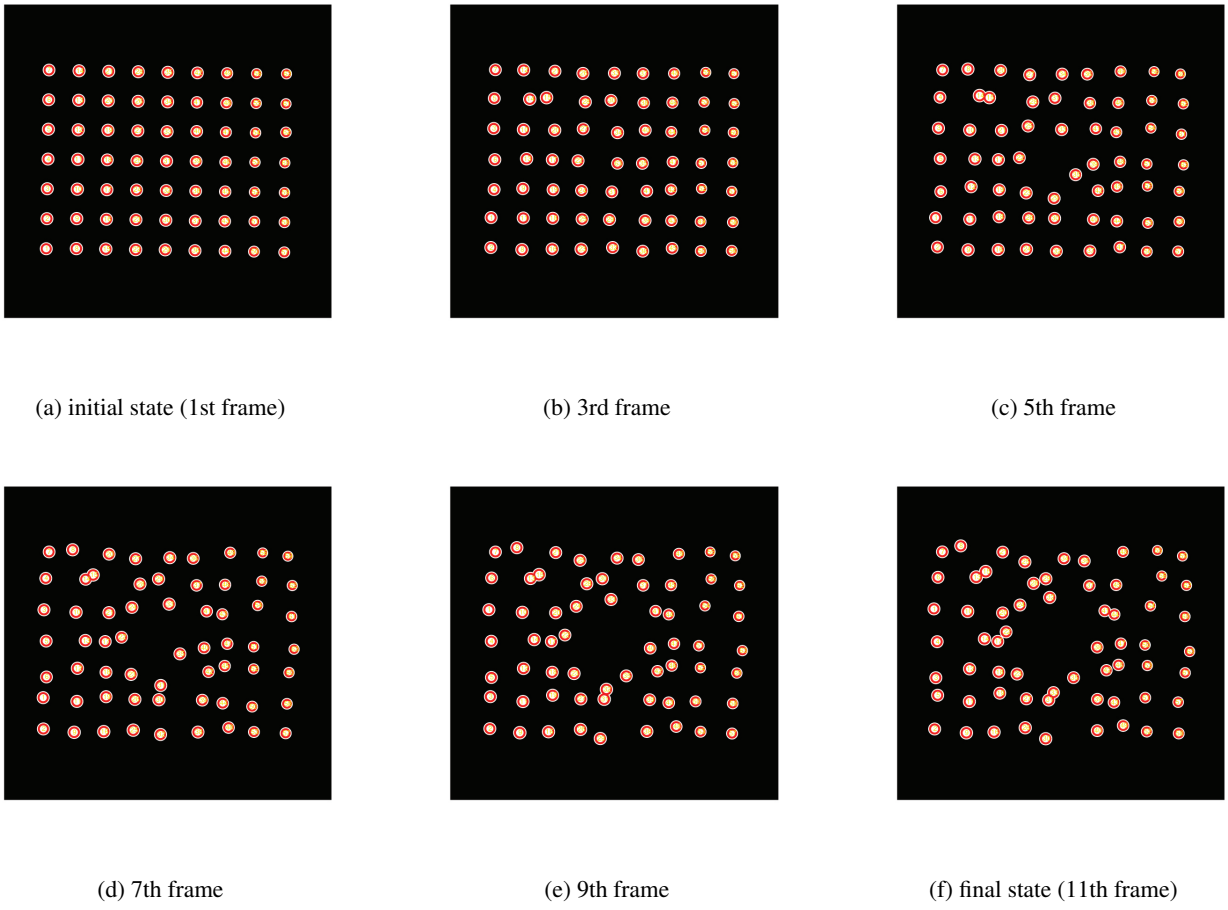

(a) initial state (1st frame) (b) 3rd frame (c) 5th frame

(d) 7th frame (e) 9th frame (f) final state (11th frame)

Fig. 2 Multiple particle motion at different stages (Trial 1)

The effect of the TR impulse is evident in these frames, where the focal region shows clear localized bead motion while beads farther away remain relatively undisturbed. Particle identity was preserved between frames using a nearest-neighbor tracking method, which enabled full trajectories to be reconstructed. The trajectories of all beads across the 11 frames are presented in fig. 3a and fig. 3d, while fig. 3b and fig. 3c compare bead displacement from the focal point, with data points color-coded by frame.

Analysis of the results highlights two important observations: First, beads located closer to the focal source consistently experienced larger displacements, confirming the localized nature of TR focusing. Second, the relationship between displacement and distance from the focal point was not strictly linear. As illustrated in fig. 3b and fig. 3c, displacement did not decrease smoothly with increasing distance; instead, localized variations were observed, where beads farther away still exhibited significant motion. Furthermore, the results from different trials indicate that the process is not strictly repeatable, as the maximum displacement reached by the center bead in the 11th frame of the first trial was already attained by the 8th frame in the second trial. These variations suggest that interference patterns and secondary reflections within the plate influence particle trajectories. The findings emphasize the complex dynamics of wave–particle coupling in elastic media and indicate that factors beyond distance alone, such as boundary conditions and scattering effects, contribute to the observed particle behavior.

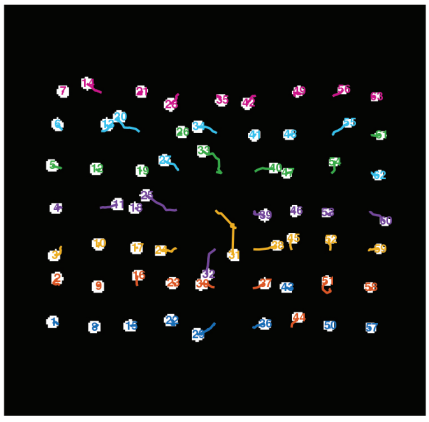

(a) Trial 1 trajectories

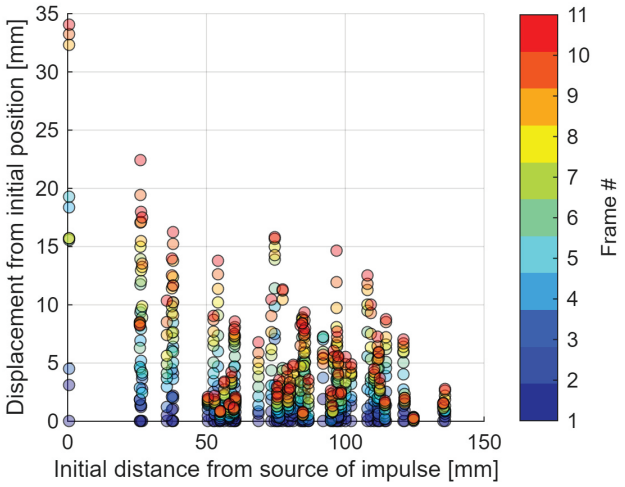

(b) Trial 1 displacement

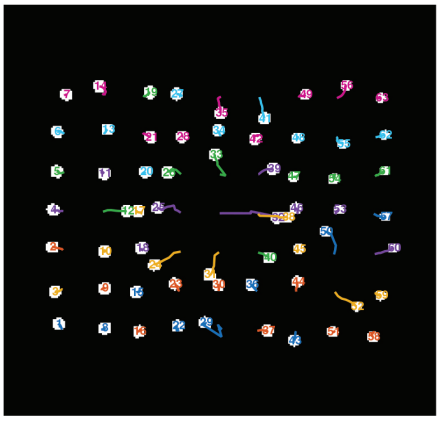

(c) Trial 2 trajectories

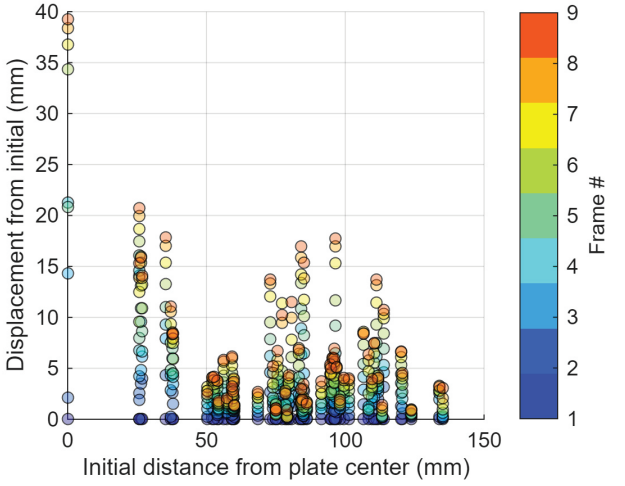

(d) Trial 2 displacement

Fig. 3 Overview of multiple particle motion: (left) reconstructed trajectories of individual beads across 11 frames, (right) displacement comparison as a function of distance from the impulse source

Conclusion

This work demonstrated the use of TR focusing to study vibration-induced particle motion on an elastic aluminum plate. The experimental setup, consisting of four modal shakers, a laser vibrometer, and an overhead camera system, successfully generated and observed TR focusing effects. Preliminary trials with a splash of water and a single bead confirmed the basic operation of the setup, while the extension to multiple particles provided a clearer view of how TR focusing influences ensembles of particles. The results showed that beads located near the focal region consistently experienced the largest displacements, confirming the localized nature of TR focusing. At the same time, the relationship between displacement and distance from the focal point was found to be non-linear, suggesting that interference patterns, reflections, and boundary effects strongly shape the observed motion.

While the experiments and modeling validate the feasibility of TR focusing for particle manipulation, several aspects remain open for further study. The model for TR focusing can be optimized by varying force and sensor locations, as well as by modifying the input signals, in order to achieve more precise and tunable focusing. The next stage of this research will include mounting the setup under a Scanning Laser Doppler Vibrometer (SLDV), which will provide a better angle for accurate measurements and yield detailed information about the vibration profile of the plate. In addition, different force positions will be simulated and tested to evaluate whether symmetry plays a role in system performance. Together, these efforts will help refine the experimental methodology and improve the control of particle motion using TR focusing.

In summary, this study establishes a foundation for applying TR-based vibration focusing to particle manipulation in elastic media. By combining experimental validation with numerical modeling, we have shown both the potential and the challenges of this approach, setting the stage for more systematic and optimized investigations in future work.

Acknowledgments This research was partially supported by the National Science Foundation through the grant CMMI-2301776.

References

1. Parvulescu, A. and Clay, C. "Reproducibility of signal transmissions in the ocean". *Radio and Electronic Engineer*, 29(4):223–228 (1965)ifnextchar.gobble.
2. Fink, M. "Time-reversed acoustics". *Scientific American*, 281(5):91–97 (1999)ifnextchar.gobble.
3. Fink, M., Cassereau, D., Derode, A., Prada, C., Roux, P., Tanter, M., Thomas, J.L., and Wu, F. "Time-reversed acoustics". *Reports on progress in Physics*, 63(12):1933 (2000)ifnextchar.gobble.
4. Fink, M., Montaldo, G., and Tanter, M. "Time-reversal acoustics in biomedical engineering". *Annual review of biomedical engineering*, 5(1):465–497 (2003)ifnextchar.gobble.
5. Thomas, J.L. and Fink, M.A. "Ultrasonic beam focusing through tissue inhomogeneities with a time reversal mirror: application to transskull therapy". *IEEE transactions on ultrasonics, ferroelectrics, and frequency control*, 43(6):1122–1129 (2002)ifnextchar.gobble.
6. Chabchoub, A. and Fink, M. "Time-reversal generation of rogue waves". *Phys. Rev. Lett.*, 112:124101 (2014)ifnextchar.gobble.
7. Prada, C., Kerbrat, E., Cassereau, D., and Fink, M. "Time reversal techniques in ultrasonic nondestructive testing of scatteringmedia". *Inverse problems*, 18(6):1761 (2002)ifnextchar.gobble.
8. de Rosny, J. and Fink, M. "Overcoming the diffraction limit in wave physics using a time-reversal mirror and a novel acoustic sink". *Phys. Rev. Lett.*, 89:124301 (2002)ifnextchar.gobble.
9. Anderson, B., Griffa, M., Ulrich, T., Le Bas, P.Y., Guyer, R., and Johnson, P. "Crack localization and characterization in solid media using time reversal techniques". In *ARMA US Rock Mechanics/Geomechanics Symposium*, pages ARMA–10. ARMA (2010)ifnextchar.gobble.
10. Anderson, B.E., Ulrich, T.J., Le Bas, P.Y., and Ten Cate, J.A. "Three-dimensional time reversal communications in elastic media". *The Journal of the Acoustical Society of America*, 139(2):EL25–EL30 (2016)ifnextchar.gobble.
11. Larmat, C.S., Guyer, R.A., and Johnson, P.A. "Time-reversal methods in geophysics". *Physics Today*, 63(8):31–35 (2010)ifnextchar.gobble.
12. Anderson, B.E., Griffa, M., Johnson, P.A., Larmat, C., and Ulrich, T.J. "Time reversal" (2008)ifnextchar.gobble.
13. Heaton, C., Anderson, B.E., and Young, S.M. "Time reversal focusing of elastic waves in plates for an educational demonstration". *The Journal of the Acoustical Society of America*, 141(2):1084–1092 (2017)ifnextchar.gobble.
14. Barnes, L.A., Anderson, B.E., Le Bas, P.Y., Kingsley, A.D., Brown, A.C., and Thomsen, H.R. "The physics of knocking over lego minifigures with time reversal focused vibrations for use in a museum exhibita)". *The Journal of the Acoustical Society of America*, 151(2):738–751 (2022)ifnextchar.gobble.
15. Draeger, C. and Fink, M. "One-channel time reversal of elastic waves in a chaotic 2d-silicon cavity". *Physical Review Letters*, 79(3):407 (1997)ifnextchar.gobble.
16. Kundu, T. *Nonlinear Ultrasonic and Vibro-Acoustical Techniques for Nondestructive Evaluation*. Springer International Publishing (2018)ifnextchar.gobble.